Multipurpose Compensation Scheme for Voltage Sag/Swell and Selective Harmonics Elimination in Distribution Systems

Mustafa INCI[1], *Mehmet BUYUK*[2], *Adnan TAN*[2],
Kamil Cagatay BAYINDIR[3], *Mehmet TUMAY*[2]

[1]Department of Mechatronics Engineering, Faculty of Engineering and Natural Sciences, Iskenderun Technical University, Gursel Mahallesi, 31200 Iskenderun/Hatay, Turkey
[2]Department of Electrical and Electronics Engineering, Faculty of Engineering and Architecture, Cukurova University, Balcali Mahallesi, Cukurova Universitesi Rektorlugu, 01330 Saricam/Adana, Turkey
[3]Department of Energy Systems Engineering, Faculty of Engineering and Natural Sciences, Ankara Yildirim Beyazit University, Ayvali Mah., Gazze Cd. No:7, 06010 Etlik-Kecioren/Kecioren/Ankara, Turkey

mustafainci63@gmail.com, mbuyuk@cu.edu.tr, atan@cu.edu.tr, kcbayindir@ybu.edu.tr, mtumay@cu.edu.tr

DOI: 10.15598/aeee.v16i1.2375

Abstract. *Voltage harmonics, sag, and swell are the most harmful disturbances in distribution systems. This paper introduces a novel effective controller method for simultaneous compensation of both voltage sag/swell and voltage harmonics by using multifunctional dynamic voltage restorer. In proposed controller method called FFT with integrated ISRF, ISRF detects the magnitudes of voltage sag/swell quickly and precisely, and FFT extracts the selective components of voltage harmonics very effectively. The proposed method integrates the superior properties of ISRF and FFT methods. FFT integrated ISRF is applied for the first time to provide the compensation of both sag/swell and selective harmonics together. The proposed system has ability to compensate symmetrical/asymmetrical sag/swell and symmetrical/asymmetrical selective harmonics which are* 5^{th}, 7^{th}, 11^{th}, *and* 13^{th}. *The controlled system is modelled in PSCAD/EMDTC and compared with conventional methods. The performance results verify that the proposed method compensates voltage disturbances effectively in the system.*

Keywords

Dynamic Voltage Restorer, FFT integrated ISRF, multifunctional compensation, sag/swell, selective voltage harmonics.

1. Introduction

Voltage, current, frequency deviations, and waveform distortions that lead to equipment failure, monetary loss, and different negative consequences are known as power quality problems in distribution systems. Sag, swell, and voltage harmonics are the most crucial power quality problems. Voltage sag is a short term drop in the amplitude of grid voltage. Short circuit faults and starting up of large loads cause voltage sag problems in distribution systems [1] and [2]. Swell is an increase in the amplitude of grid voltage. Voltage swell is not as widespread as voltage sag, but it could be more harmful and destructive [3]. Voltage harmonics distortion defined as a distortion of the fundamental sinusoidal voltage waveform alternating at 50/60 Hz and repeats in every cycle [4]. While sag/swell causes the damage of electronic equipment and failure of systems, voltage harmonics induce overheating and losses in cables, transformers, and motors. There are various custom power devices to cope with these problems in distribution systems. Among these devices, Dynamic Voltage Restorer (DVR) is the most effective device to compensate these power quality problems. DVR is an inverter based structure which is located between sensitive load and grid in the system. The main components in a conventional DVR are inverter, dc-link capacitor, filter, and injection transformer [5], [6] and [7]. DVR injects controlled voltage in series to mitigate the influence of voltage disturbances on sensitive loads.

The main functionality of a conventional DVR is to compensate only sag/swell problems in the system

[8]. In the literature, DVRs have been recently applied to compensate both sag/swell and voltage harmonics, which are also named as multifunctional DVRs. Table 1 shows the compensation capabilities of multifunctional DVRs in [9], [10], [11], [12], [13], [14], [15], [16], [17], [18], [19] and [20]. Besides, these studies employ several reference generation methods to compensate multiple voltage disturbances at the same time. Among these studies, [11] and [15] examine the mitigation of only symmetrical voltage harmonics with sag/swell compensation. In addition, Instantaneous power theory and Perceptron based control algorithm are used for alleviation of symmetrical/asymmetrical sag/swell and only symmetrical voltage harmonics. In [12], the most common topology called as SRF theory which transforms 3-φ voltages to d-q components is used for symmetrical sag/swell and voltage harmonics. The asymmetrical problems of sag/swell and voltage harmonics are compensated in [20] by using ISRF.

This paper presents a novel reference generation method based on Fast Fourier Transform (FFT) with integrated Improved Synchronous Reference Frame (ISRF) in order to compensate sag/swell with selective voltage harmonics via multifunctional DVR. The ISRF method applied in this study is more accurate and fast among sag/swell detection techniques. In addition, FFT is very effective approach to extract the components of voltage harmonics. This method shows superior properties of ISRF and FFT. The proposed FFT with integrated ISRF method is applied for the first time to compensate both sag/swell and asymmetrical selective voltage harmonics, simultaneously.

Tab. 1: Compensation capabilities of multifunctional DVRs in literature studies and the proposed study.

Compensation Capability	Study
Symmetrical voltage sag/swell	[10]
Symmetrical/asymmetrical voltage sag/swell	[9], [14], [16] and [19]
Symmetrical/asymmetrical voltage sag and symmetrical voltage harmonics	[13], [17] and [18]
Symmetrical voltage sag/swell and symmetrical voltage harmonics	[12]
Symmetrical/asymmetrical voltage sag/swell and only symmetrical harmonics	[11] and [15]
Symmetrical/asymmetrical voltage sag/swell and all components of symmetrical/asymmetrical voltage harmonics	[20]
Symmetrical/asymmetrical voltage sag/swell and symmetrical/asymmetrical selective voltage harmonics	proposed study

In the proposed study:

- The main contribution of this study is the elimination of symmetrical/asymmetrical sag/swell and symmetrical/asymmetrical voltage harmonics, simultaneously.
- ISRF is selected for compensation of sag/swell due to the fast speed detection property.

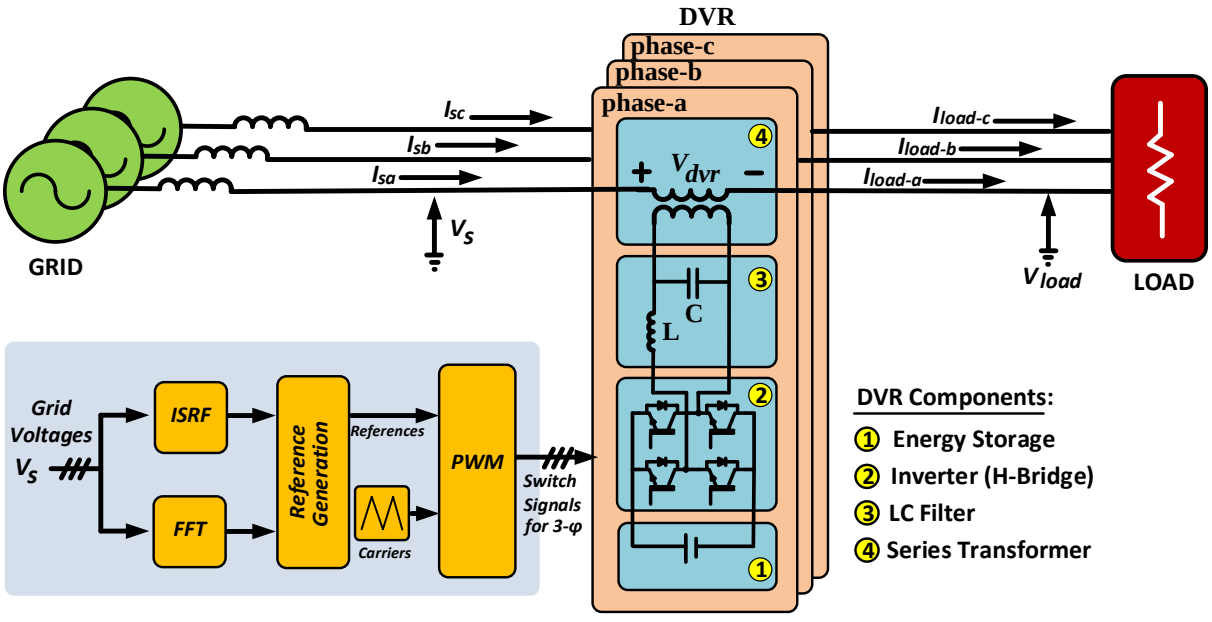

Fig. 1: Proposed reference signal generation based on FFT with integrated ISRF method and Dynamic Voltage Restorer.

- Harmonic compensation is achieved by using FFT method instead of ISRF.
- FFT achieves compensation of both symmetrical and asymmetrical voltage harmonics.
- The system has ability to compensate up to 30 % sag/swell with the attenuation of selective voltage harmonics which are 5^{th}, 7^{th}, 11^{th}, and 13^{th}.

2. FFT Integrated ISRF

DVRs, which are connected between grid and sensitive load, are implemented to inject controlled voltage in series to prevent adverse influence of voltage issues on sensitive loads [20], [21], [22] and [23]. Figure 1 shows the proposed reference generation method for multi-functional DVR.

The control strategy is a fairly critical issue in DVR. The primary purpose of the control system is to compensate sag/swell problems and to attenuate the effects of voltage harmonics in distorted grid voltages. Voltage detection is one of the most important subjects in a control system. Many voltage detection methods are presented with different control algorithms in literature. Sag/swell and harmonics must be compensated rapidly and accurately.

The flow chart of FFT with integrated ISRF is presented in Fig. 2. According to the proposed controller, grid voltages are firstly measured and converted to per unit (pu) values. In the next step, the per unit signals are used to generate the magnitudes of fundamental component and selective harmonics signals by using ISRF and FFT methods, respectively. Then, the mathematical processes are performed to produce reference signals for sag/swell and harmonics. Finally, reference signal is obtained and compared with carrier signal in Pulse Width Modulation (PWM), and switching signals for IGBTs in inverter are generated to inject controlled voltage in series for compensation.

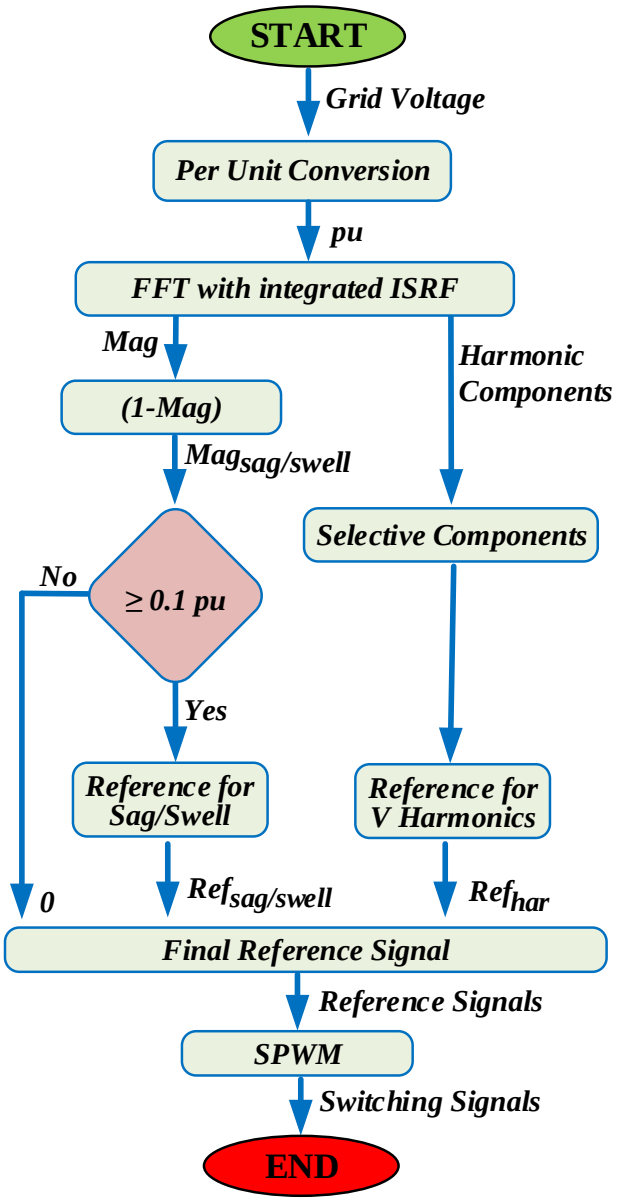

Fig. 2: Flowchart of FFT integrated ISRF for mitigation of multiple voltage *disturbances*.

2.1. Sag/Swell Detection: ISRF

Conventional SRF theory or dq-transformation cannot achieve detection of voltage disturbances under asymmetrical condition. In order to eliminate the drawback of conventional SRF, different approaches have been developed. Conventional dq-transformation is not feasible for a single phase voltage measurement because of 3-φ information that is used at the same time. Therefore, this transform process causes inaccurate voltage detection under asymmetrical (unbalanced) conditions. In this study, ISRF method is used to detect sag/swell signals in asymmetrical conditions, as shown in Fig. 3. In this study, ISRF eliminates the requirement of other phases to generate magnitude information for single-phase. In proposed method, dq transform is realized for each phases, separately. To apply dq transform for each phase voltage, three symmetric virtual signals can be produced by a single voltage (for example phase-a) [20], which is transformed into dq transform given in Eq. (1), Eq. (2) and Eq. (3). Virtual signals for second input (In_2) and third input (In_3) in dq transform are generated applying mathematical equations on actual input (In_1). These processes are separately executed for all phases.

In conventional dq transformation, the input voltages must be equal to $\frac{2\pi}{3}$ rad phase difference to detect voltage signals accurately. There is a relationship be-

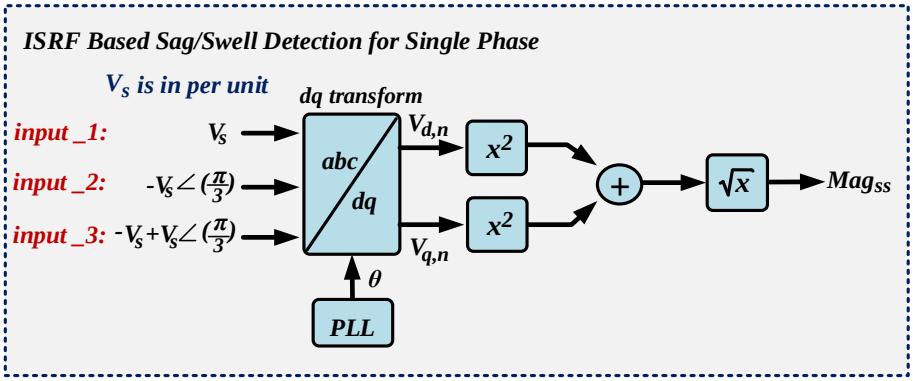

Fig. 3: ISRF method for a single phase.

tween interconnection of phases in a 3-φ system. Relationship between symmetrical 3-φ voltages are expressed by Eq. (1), Eq. (2) and Eq. (3):

$$In_1 = V_s\angle\left(0\right), \tag{1}$$

$$In_2 = V_s\angle\left(\frac{2\pi}{3}\right), \tag{2}$$

$$In_3 = V_s\angle\left(\frac{2\pi}{3}\right). \tag{3}$$

In ISRF method, virtual signals are generated by using only single phase information [20], as shown in Fig. 3. This operation is performed separately for all phases in multiple frame. According to Eq. (1), Eq. (2) and Eq. (3), the application of these signals in dq transform gives slow response for detection of voltage sag/swell. In order to achieve faster detection, virtual signals for In_2 and In_3 are reproduced by using a single voltage. These signals are expressed in Eq. (4) and Eq. (5). π is equal to -1 in phasor form and $\frac{4\pi}{3}$ is obtained by the multiplication of $\frac{\pi}{3}$ and -1. In this way, In_2 is generated virtually by delay of $\frac{\pi}{3}$. In a balanced system, the sum of phasor voltages is zero ($In_1 + In_2 + In_3 = 0$). As a result, In_3 is defined as the negative of the sum of In_1 and In_2.

$$In_2 = V_s\angle\left(-\frac{2\pi}{3}\right) = V_s\angle\left(\frac{4\pi}{3}\right) = -V_s\angle\left(\frac{\pi}{3}\right), \tag{4}$$

$$In_3 = -\left(In_1 + In_2\right) = -V_s + V_s\angle\left(\frac{\pi}{3}\right). \tag{5}$$

In ISRF, In_1 and its virtual signals (In_2 and In_3) are firstly transformed into α and β components for each phase in multiple frames.

$$\begin{pmatrix} V_{\alpha,n} \\ V_{\beta,n} \\ V_{0,n} \end{pmatrix} = \sqrt{\frac{2}{3}} \begin{pmatrix} 1 & -\frac{1}{2} & -\frac{1}{2} \\ 0 & \frac{\sqrt{3}}{2} & -\frac{\sqrt{3}}{2} \\ \frac{1}{\sqrt{2}} & \frac{1}{\sqrt{2}} & \frac{1}{\sqrt{2}} \end{pmatrix} \begin{pmatrix} In_1 \\ In_2 \\ In_3 \end{pmatrix}. \tag{6}$$

In the next step, α-β components are converted to dq components according Eq. (7).

$$\begin{pmatrix} V_{d,n} \\ V_{q,n} \end{pmatrix} = \begin{pmatrix} \cos\left(\omega t\right) & \sin\left(\omega t\right) \\ -\sin\left(\omega t\right) & \cos\left(\omega t\right) \end{pmatrix} \begin{pmatrix} V_{\alpha,n} \\ V_{\beta,n} \end{pmatrix}, \quad n = a, b, c. \tag{7}$$

In dq reference frame, d- and q- components are orthogonal signals and used to define the magnitude of a single phase voltage via proposed controller. The square root of sum of squares of d- and q- components in Eq. (8) gives the magnitude for a single-phase voltage.

$$Mag_{ss,n} = \sqrt{V_{d,n}^2 + V_{q,n}^2}, \quad n = a, b, c. \tag{8}$$

In sag/swell detection, magnitude of voltage sag/swell in pu (Mag_{ss}) is extracted from ISRF. Measured magnitude signal (Mag_{ss}) is extracted from 1 pu to calculate the depth of sag/swell (SS_{depth}).

$$SS_{depth} = 1 - Mag_{ss}. \tag{9}$$

2.2. Detection of Selective Voltage Harmonics: FFT

Several harmonic detection methods have been applied in power quality applications in literature. In this study, FFT based harmonic detection technique in [24] is used to obtain the harmonics of the grid voltage. The FFT, which consists of small Discrete Fourier Transform (DFT) components has a rapid response due to less complex calculations. Among FFT techniques, Cooley-Tukey is the most commonly applied algorithm [25] and [26], as illustrated in Fig. 4. The DFT form of the grid voltage is defined as

$$V\left[k\right] = \sum_{n=0}^{N-1} v(n) W^{nk}, \quad k = 0, 1, 2, \ldots, N-1, \tag{10}$$

where k is the harmonic frequency index, N is the number of sampling points, $W^k = e^{-j2\pi k/N}$. The Eq. (10) can be written in polar form as

$$V\left[k\right] = V_m\left(k\right) e^{j\theta(k)}, \tag{11}$$

where V_m and θ indicate the magnitude and phase angle of k-th harmonic, respectively.

In Cooley-Tukey algorithm, the voltage samples are categorized as odd samples $(2n+1)$ and even samples $(2n)$ [26]. Thus, Eq. (10) can be rewritten as

$$V[k] = \sum_{n=0}^{\frac{N}{2}-1} v(2n)W^{2nk} + W^k \sum_{n=0}^{\frac{N}{2}-1} v(2n+1)W^{2nk}, \quad (12)$$

where $W_N^{2nk} = e^{-j\frac{2\pi}{N}2nk} = e^{-j\frac{2\pi}{N/2}nk} = W_{N/2}^{nk}$.

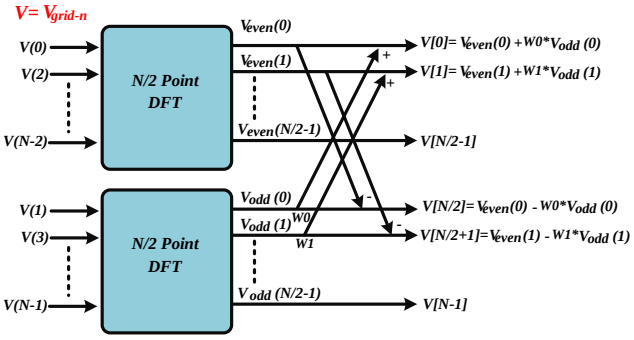

Fig. 4: $N/2$-point DFTs approach of FFT.

By substituting $W_{N/2}^{nk}$ by W_N^{2nk}, the Eq. (12) becomes

$$V[k] = \underbrace{\sum_{n=0}^{\frac{N}{2}-1} v(2n)W_{\frac{N}{2}}^{nk}}_{V_{even}(k)} + \underbrace{W^k \sum_{n=0}^{\frac{N}{2}-1} v(2n+1)W_{\frac{N}{2}}^{nk}}_{V_{odd}(k)}, \quad (13)$$

$$V[k] = V_{even}(k) + W^k V_{odd}(k). \quad (14)$$

By using symmetric $\left(W_N^{k+\frac{N}{2}} = -W_N^k\right)$ and periodic $\left(W_{\frac{N}{2}}^{k+\frac{N}{2}} = W_{\frac{N}{2}}^k\right)$ properties, Eq. (13) becomes

$$V\left[k+\frac{N}{2}\right] = \underbrace{\sum_{n=0}^{\frac{N}{2}-1} v(2n)W_{\frac{N}{2}}^{nk}}_{V_{even}(k)} - \underbrace{W^k \sum_{n=0}^{\frac{N}{2}-1} v(2n+1)W_{\frac{N}{2}}^{nk}}_{V_{odd}(k)}, \quad (15)$$

$$V\left[k+\frac{N}{2}\right] = V_{even}(k) - W^k V_{odd}(k). \quad (16)$$

The $N/2$-point DFTs can be reduced by $N/4$-point DFTs in order to reduce the computational cost. If the sample number is selected as the power of 2 ($N = 2r$), then it can be degraded until 2-point DFTs which is known as radix-2 FFT algorithm. Therefore, the calculations are decreased, and FFT becomes faster. In this study, 1024 points are exploited in 1-period. As a result, radix-2 FFT algorithm is applied as illustrated in Fig. 5.

2.3. Reference Signal Generation

Figure 6 shows reference signal generation method using ISRF and FFT, simultaneously. While ISRF is

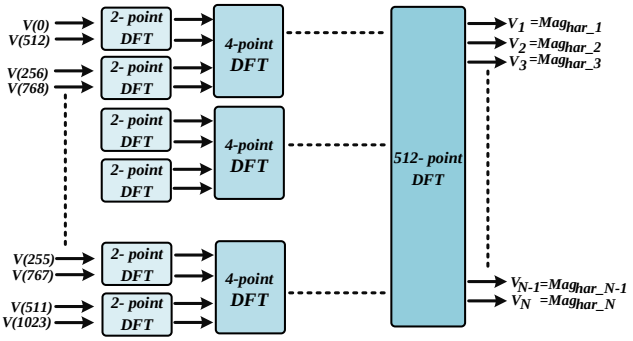

Fig. 5: Radix-2 FFT with 1024 samples of the grid voltage.

employed to calculate the depth of sag/swell, FFT extracts the 5th, 7th, 11th, and 13th harmonic components.

Reference signal of sag/swell (Ref_{ss}) is in phase with grid-side voltage. In order to determine Ref_{ss}, the depth value of sag/swell is multiplied by a sine function in-phase with grid-side voltage. In this way, reference signal of sag/swell is determined as

$$Ref_{ss}(n) = (1 - Mag_{ss}) \angle \left(\theta - \frac{\pi}{2}\right), \quad n = a, b, c, \quad (17)$$

where θ_n is instantaneous phase angle.

To generate reference signal of voltage harmonics, FFT extracts the selective components (5th, 7th, 11th, and 13th) of voltage harmonics for each phase, separately:

$$Ref_{har}(n) = \sum_{N \subset M} Mag_{har,N} \sin(wt + \theta_N), \quad (18)$$

where $M = 5, 7, 11, 13$.

In order to compensate voltage harmonics, the inverse voltage is supplied to the grid. As a result, reference signal is the summation of Ref_{ss} and negative Ref_{har}:

$$Reference(n) = Ref_{ss}(n) - Ref_{har}(n) = \quad (19)$$

$$(1 - Mag_{ss}) \sin(wt + \theta) - \sum_{N \subset M} Mag_{har,N} \sin(wt + \theta_N),$$

where M indicates 5, 7, 11, and 13.

The final reference signal is compared with carrier signals in Sinusoidal PWM to generate controlled voltages for compensation process.

3. Case Studies

In this section, performance results of the proposed method based on ISRF and FFT are presented for application in multifunctional DVR system. The system includes a sensitive load which has a capacity of

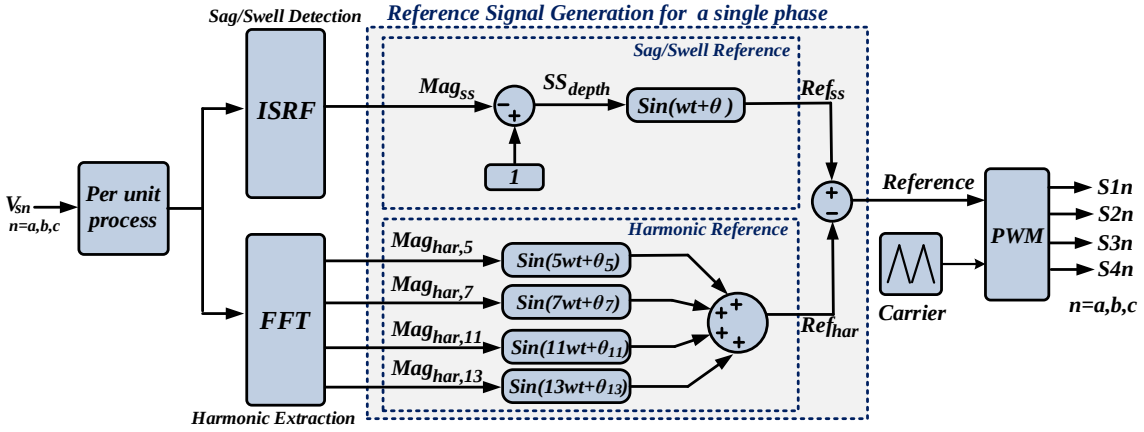

Fig. 6: Proposed reference signal generation for voltage sag/swell and selective voltage harmonics.

1 MVA. It is fed from 690 Vrms (peak value of phase voltage is 560 V) 3-φ supply. The system parameters are given in Tab. 2. The proposed DVR is designed to compensate up to 30 % 3-φ sag and selective voltage harmonics (5^{th}, 7^{th}, 11^{th}, and 13^{th}) at different grid-side THD values. The system and proposed controller model is implemented in PSCAD/EMTDC to compensate sag/swell and selective voltage harmonics at the grid side.

Tab. 2: System parameters.

	Parameter	Value
Source	Fundamental Frequency	50 Hz
	Source Voltage	690 V (line-line, rms voltage)
DVR	Compensation Rating	30 %
	Power Rating	300 kVA
	Transformer Turn ratio	10/3
	DC-link Voltage	800 V
	Filter Inductor (Lf)	0.1 mH
	Filter Capacitor (Cf)	30 µF
	Filter Resistance (Rf)	0.05 Ω

Different case studies are analysed using PSCAD/EMDTC to verify the controller method. These case studies are:

- Case I: Performance comparison of SRF and ISRF for asymmetrical sag detection.
- Case II: Simultaneous compensation of:
  - symmetrical selective voltage harmonics and symmetrical sag,
  - symmetrical selective voltage harmonics and asymmetrical swell.
- Case III: Simultaneous compensation of:
  - asymmetrical selective voltage harmonics and asymmetrical sag,
  - asymmetrical selective voltage harmonics and asymmetrical swell.

Firstly, the performance results of ISRF and conventional SRF are compared for asymmetrical sag cases. As shown in Fig. 7, ISRF is applicable for asymmetrical sag conditions while conventional SRF cannot achieve accurate detection (Case I). ISRF detects sags fast and accurately within 1.3 ms, 2.4 ms, and 0.3 ms for phase-a, phase-b, and phase-c, respectively.

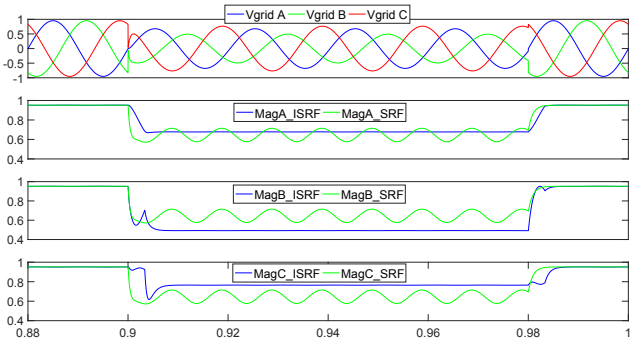

Fig. 7: Performance comparison of SRF and ISRF.

Table 3 and Tab. 4 shows the THD values before/after compensation for Case II and Case III, respectively. Harmonic compensation capabilities of ISRF and FFT was compared. In Case II, the system was used for compensation of symmetrical voltage harmonics and symmetrical sag/asymmetrical single phase swell at same time. In Case II-A, 3-φ sag occurs at 0.3 s for 5 periods, and the peak value of 3-φ voltages is reduced to 392 (0.7 pu) from 560 V (1 pu) in addition to voltage harmonics compensation. DVR compensates 0.3 pu sag, and THD values of load voltages are diminished to 2.14 %, 2.21 %, and 2.03 % from 11.38 % for phase-a, phase-b, and phase-c, respectively. Figure 8(a) shows voltage waveforms of grid-side, injected, and load-side voltages. In Case II-B, single phase voltage swell condition occurs during five periods. The peak value of grid side voltage increases to 672 V (1.2 pu) from 560 V (1 pu) at phase-c. The compensation of 20 % single phase swell and symmetrical selective voltage harmonics are presented in Fig. 8(b).

Tab. 3: THD and harmonic values of case studies before/after compensation-symmetrical condition.

		Symmetrical Condition (%)		
		Before Compensation	ISRF	FFT
Phase A	THD	11.36	2.97	2.14
	5^{th}	8.29	1.49	1.29
	7^{th}	5.97	2.22	0.12
	11^{th}	3.78	1.03	0.22
	13^{th}	3.25	0.76	0.31
Phase B	THD	11.36	2.88	2.21
	5^{th}	8.29	1.61	0.96
	7^{th}	5.97	1.95	0.25
	11^{th}	3.78	1.06	0.27
	13^{th}	3.25	0.83	0.68
Phase C	THD	11.36	3.22	2.03
	5^{th}	8.29	1.83	1.33
	7^{th}	5.97	2.06	0.72
	11^{th}	3.78	0.49	0.29
	13^{th}	3.25	0.75	0.49

Tab. 4: THD and harmonic values of case studies before/after compensation-asymmetrical condition.

		Asymmetrical Condition (%)		
		Before Compensation	ISRF	FFT
Phase A	THD	9.81	2.42	1.49
	5^{th}	7.2	1.68	0.77
	7^{th}	5.24	1.21	0.54
	11^{th}	3.24	0.63	0.23
	13^{th}	2.52	0.49	0.3
Phase B	THD	7.98	2.14	1.62
	5^{th}	5.94	1.26	0.81
	7^{th}	4.15	1.33	0.42
	11^{th}	2.53	0.73	0.42
	13^{th}	2.16	0.29	0.22
Phase C	THD	10.08	2.95	1.78
	5^{th}	7.93	1.62	1.22
	7^{th}	5.61	1.47	0.79
	11^{th}	3.6	0.88	0.49
	13^{th}	3.07	0.68	0.47

In Fig. 9, individual harmonic spectrum before/after compensation is presented for Case II.

Case III-A and Case III-B present asymmetrical voltage harmonics (THDA = 9.81 %, THDB = 7.98 %, and THDC = 10.8 %) which distort voltage waveforms. Two phase asymmetrical sag and asymmetrical voltage harmonics condition (Case III-A) at grid-side is presented in Fig. 10(a). In single phase fault, voltage value of phase-a decreases to 0.7 pu from 1 pu during the period of 0.9–1.0 s. Besides, different THD values appear at grid-side: 9.81 % at phase-a, 7.98 % at phase B, and 10.8 % at phase-c, respectively. In this case, both asymmetrical selective voltage harmonics and asymmetrical single phase sag is compensated at the same time. THD value at load-side is reduced to 1.49 % at phase-a, 1.62 % at phase-b, and 1.78 % at phase-c, respectively. In Case III-B, 3-φ asymmetrical voltage swell occurs from 1.3 s to 1.4 s, as shown in Fig. 10(b). The peak value of grid side voltage increases to 672 V (1.2 pu), 700 V (1.25 pu), 644 V (1.15 pu) from 560 V

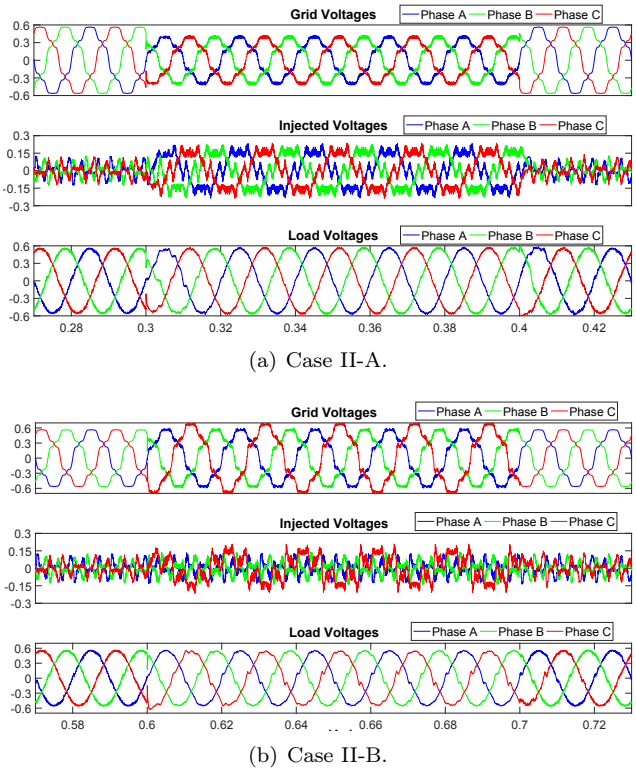

(a) Case II-A.

(b) Case II-B.

Fig. 8: Waveforms of grid-side, injected, and load-side voltages.

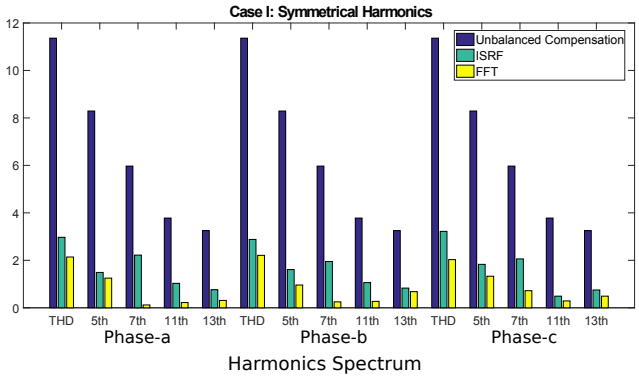

Fig. 9: THD values under balanced voltage harmonics before/after compensation for Case II.

(1 pu) at phase-a, phase-b, and phase-c, respectively. In Fig. 11, individual harmonic spectrum before/after compensation is presented for Case III.

4. Conclusion

In this study, a novel reference generation method based on ISRF and FFT is introduced for detection of sag/swell and extraction of voltage harmonics. Symmetrical/asymmetrical sag/swell and symmetrical/asymmetrical selective voltage harmonics are compensated by using the proposed method. Performance results of 30 % sag and 25 % voltage swell

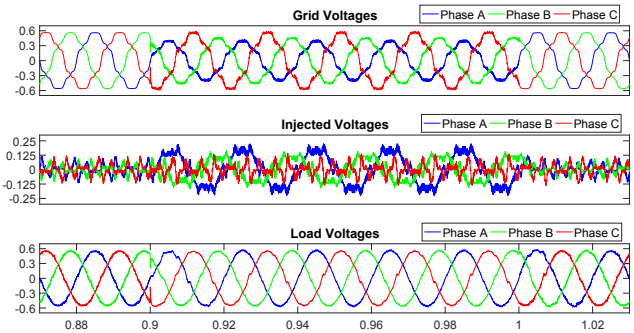

(a) Case III-A.

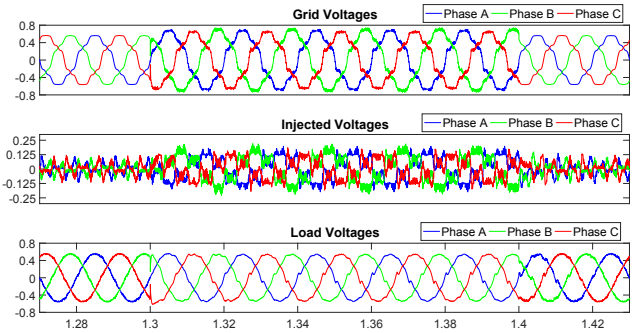

(b) Case III-B.

Fig. 10: Waveforms of grid-side, injected and load-side voltages.

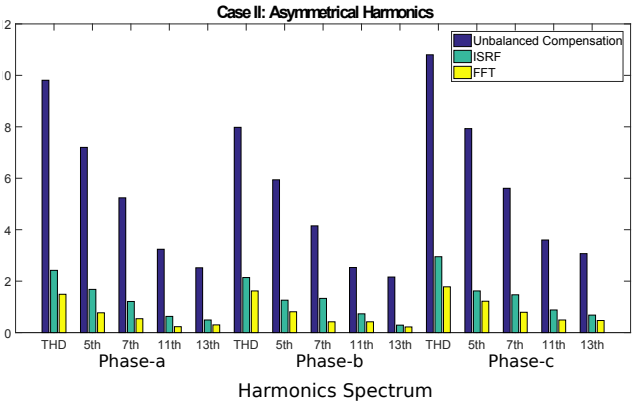

Fig. 11: THD values under unbalanced voltage harmonics before/after compensation for Case III.

compensation are analyzed in addition to asymmetrical selective voltage harmonics (5^{th}, 7^{th}, 11^{th}, and 13^{th}). THD level in system is reduced nearly to 2 % from 12.36 % with the proposed controller. The case studies verify that the proposed method performs very effectively and compensates voltage disturbances in the system.

Acknowledgment

This study is financially supported by TUBITAK (Project Number: 115R304).

References

[1] HEINE, P. and M. LEHTONEN. Voltage sag distributions caused by power system faults. *IEEE Transactions on Power Systems*. 2003, vol. 18, iss. 4, pp. 1367–1373. ISSN 0885-8950. DOI: 10.1109/Tpwrs.2003.818606.

[2] NOROUZI, M. A., J. OLAMAEI and G. B. GHAREHPETIAN. Compensation of voltage sag and flicker during thermal power plant turbo-expander operation by dynamic voltage restorer. *International Transactions on Electrical Energy Systems*. 2016, vol. 26, iss. 1, pp. 16–31. ISSN 2050-7038. DOI: 10.1002/etep.2063.

[3] BURGOS, R. P. and E. P. WIECHMANN. Extended voltage swell ride-through capability for PWM voltage-source rectifiers. *IEEE Transactions on Industrial Electronics*. 2005, vol. 52, iss. 4, pp. 1086–1098. ISSN 0278-0046, DOI: 10.1109/Tie.2005.851643.

[4] SINGH, G. K. Power system harmonics research: a survey. *European Transactions on Electrical Power*. 2009, vol. 19, iss. 2, pp. 151–172. ISSN 1546-3109. DOI: 10.1002/etep.201.

[5] RAUF, A. M. and V. KHADKIKAR. An Enhanced Voltage Sag Compensation Scheme for Dynamic Voltage Restorer. *IEEE Transactions on Industrial Electronics*. 2015, vol. 62, iss. 5, pp. 2683–2692. ISSN 0278-0046. DOI: 10.1109/Tie.2014.2362096.

[6] RAUF, A. M. and V. KHADKIKAR. Integrated Photovoltaic and Dynamic Voltage Restorer System Configuration. *IEEE Transactions on Sustainable Energy*. 2015, vol. 6, iss. 2, pp. 400–410. ISSN 1949-3029. DOI: 10.1109/Tste.2014.2381291.

[7] TAGHIZADEH, S., N. MEI LIN TAN and M. KARIMI-GHARTEMANI. Study of fuzzy based control algorithm for dynamic voltage restorer. *International Transactions on Electrical Energy Systems*. 2015, vol. 25, iss. 12, pp. 3600–3617. ISSN 2050-7038. DOI: 10.1002/etep.2055.

[8] INCI, M., K. C. BAYINDIR and M. TUMAY. The performance improvement of dynamic voltage restorer based on bidirectional dc–dc converter. *Electrical Engineering*. 2017,

vol. 99, iss. 1, pp. 285–300. ISSN 1432-0487. DOI: 10.1007/s00202-016-0422-1.

[9] CARLOS, G. A. A., E. C. DOS SANTOS, C. B. JACOBINA and J. P. R. A. MELLO. Dynamic Voltage Restorer Based on Three-Phase Inverters Cascaded Through an Open-End Winding Transformer. *IEEE Transactions on Power Electronics*. 2016, vol. 31, iss. 1, pp. 188–199. ISSN 0885-8993. DOI: 10.1109/Tpel.2015.2404798.

[10] CHEN, G. D., M. ZHU and X. CAI. Medium-voltage level dynamic voltage restorer compensation strategy by positive and negative sequence extractions in multiple reference frames. *IET Power Electronics*. 2014, vol. 7, iss. 7, pp. 1747–1758. ISSN 1755-4535. DOI: 10.1049/iet-pel.2013.0520.

[11] ELNADY, A. and M. M. A. SALAMA. Mitigation of voltage disturbances using adaptive perceptron-based control algorithm. *IEEE Transactions on Power Delivery*. 2005, vol. 20, iss. 1, pp. 309–318. ISSN 0885-8977. DOI: 10.1109/Tpwrd.2004.835036.

[12] JAYAPRAKASH, P., B. SINGH, D. P. KOTHARI, A. CHANDRA and K. AL-HADDAD. Control of Reduced-Rating Dynamic Voltage Restorer With a Battery Energy Storage System. *IEEE Transactions on Industry Applications*. 2014, vol. 50, iss. 2, pp. 1295–1303. ISSN 0093-9994. DOI: 10.1109/Tia.2013.2272669.

[13] JOWDER, F. A. L. Design and analysis of dynamic voltage restorer for deep voltage sag and harmonic compensation. *IET Generation Transmission & Distribution*. 2009, vol. 3, iss. 6, pp. 547–560. ISSN 1751-8687. DOI: 10.1049/iet-gtd.2008.0531.

[14] LAM, C.-S., M.-C. WONG and Y.-D. HAN. Voltage Swell and Overvoltage Compensation With Unidirectional Power Flow Controlled Dynamic Voltage Restorer. *IEEE Transactions on Power Delivery*. 2008, vol. 23, iss. 4, pp. 2513–2521. ISSN 0885-8977. DOI: 10.1109/Tpwrd.2008.921142.

[15] LEE, S.-J., H. KIM, S.-K. SUL and F. BLAABJERG. A novel control algorithm for static series compensators by use of PQR instantaneous power theory. *IEEE Transactions on Power Electronics*. 2004, vol. 19, iss. 3, pp. 814–827. ISSN 0885-8993. DOI: 10.1109/Tpel.2004.826499.

[16] LI, G. J., X. P. ZHANG, S. S. CHOI, T. T. LIE, and Y. Z. SUN. Control strategy for dynamic voltage restorers to achieve minimum power injection without introducing sudden phase shift. *IET Generation Transmission & Distribution*. 2007, vol. 1, iss. 5, pp. 847–853. ISSN 1751-8687. DOI: 10.1049/iet-gtd:20060494.

[17] NEWMAN, M. J., D. G. HOLMES, J. G. NIELSEN and F. BLAABJERG. A dynamic voltage restorer (DVR) with selective harmonic compensation at medium voltage level. *IEEE Transactions on Industry Applications*. 2005, vol. 41, iss. 6, pp. 1744–1753. ISSN 0093-9994. DOI: 10.1109/Tia.2005.858212.

[18] RONCERO-SANCHEZ, P., E. ACHA, J. E. ORTEGA-CALDERON, V. FELIU and A. GARCIA-CERRADA. A Versatile Control Scheme for a Dynamic Voltage Restorer for Power-Quality Improvement. *IEEE Transactions on Power Delivery*. 2009, vol. 24, iss. 1, pp. 277–284. ISSN 0885-8977. DOI: 10.1109/Tpwrd.2008.2002967.

[19] SOMAYAJULA, D. and M. L. CROW. An Integrated Dynamic Voltage Restorer-Ultracapacitor Design for Improving Power Quality of the Distribution Grid. *IEEE Transactions on Sustainable Energy*. 2015, vol. 6, iss. 2, pp. 616–624. ISSN 1949-3029. DOI: 10.1109/Tste.2015.2402221.

[20] INCI, M., K. C. BAYINDIR and M. TUMAY. Improved Synchronous Reference Frame based controller method for multifunctional compensation. *Electric Power Systems Research*. 2016, vol. 141, iss. 1, pp. 500–509. ISSN 0378-7796. DOI: 10.1016/j.epsr.2016.08.033.

[21] KHOSHKBAR SADIGH, A. and K. M. SMEDLEY. Fast and precise voltage sag detection method for dynamic voltage restorer (DVR) application. *Electric Power Systems Research*. 2016, vol. 130, iss. 1, pp. 192–207. ISSN 0378-7796. DOI: 10.1016/j.epsr.2015.08.002.

[22] EBRAHIMZADEH, E., S. FARHANGI, H. IMAN-EINI, F. B. AJAEI and R. IRAVANI. Improved Phasor Estimation Method for Dynamic Voltage Restorer Applications. *IEEE Transactions on Power Delivery*. 2015, vol. 30, iss. 3, pp. 1467–1477. ISSN 0885-8977. DOI: 10.1109/Tpwrd.2014.2366241.

[23] NAIDU, S. R. and D. A. FERNANDES. Dynamic voltage restorer based on a four-leg voltage source converter. *IET Generation Transmission & Distribution*. 2009, vol. 3, iss. 5, pp. 437–447. ISSN 1751-8687. DOI: 10.1049/iet-gtd.2008.0411.

[24] WANG, J., X. HU and S. CHEN. Research on detection algorithm of voltage sag characteristics. In: *7th IEEE Conference on Industrial Electronics and Applications*. Singapore:

IEEE, 2012, pp. 313–318. ISBN 978-1-4577-2118-2. DOI: 10.1109/ICIEA.2012.6360743.

[25] ASIMINOAEI, L., F. BLAABJERG and S. HANSEN. Evaluation of harmonic detection methods for active power filter applications. In: *Twentieth Annual IEEE Applied Power Electronics Conference and Exposition*. Austin: IEEE, 2005, pp. 635–641. ISBN 0-7803-8975-1. DOI: 10.1109/APEC.2005.1453014.

[26] SARIBULUT, L., A. TEKE and M. TUMAY. Fundamentals and literature review of Fourier transform in power quality issues. *Journal of Electrical and Electronics Engineering Research*. 2013, vol. 5, iss. 1, pp. 9–22. ISSN 1993-8225. DOI: 10.5897/JEEER2013.0436.

About Authors

Mustafa INCI received the M.Sc. and Ph.D. degree in Electrical and Electronics Engineering from Cukurova University, Adana, Turkey. His research interests include power quality, grid connected wind energy systems, multilevel inverters, and advanced modulation techniques.

Mehmet BUYUK received his B.Sc. and M.Sc. from Electrical and Electronics Engineering Department of Cukurova University, Adana, Turkey, in 2012 and 2015, respectively. Now, he has been working as research assistant in Electrical and Electronics Engineering Department of Cukurova University since 2014. His research interests include power quality and multilevel inverters.

Adnan TAN received the Ph.D. degree in Electrical and Electronics Engineering from Cukurova University, Adana, Turkey. Currently he is an Assistant Professor of the Electrical and Electronics Engineering Department, Cukurova University, Adana, Turkey. His research interests include modelling of electrical machines, power flow controllers, power quality, and custom power devices.

Kamil Cagatay BAYINDIR received the Ph.D. degree in Electrical and Electronics Engineering from Cukurova University, Adana, Turkey. Currently he is an Associate Professor of the Electrical and Electronics Engineering Department, Yildimir Beyazit University, Ankara, Turkey. His research interests include modelling of electrical machines, power flow controllers, power quality, and custom power devices.

Mehmet TUMAY received the Ph.D. degree in Electrical Engineering from Strathclyde University, Glasgow, UK, in 1995. Currently, he is a Professor at the Electrical and Electronics Engineering Department, Cukurova University, Adana, Turkey. His research interests include modelling of electrical machines, power flow controllers, power quality, and custom power devices.